

See discussions, stats, and author profiles for this publication at: <https://www.researchgate.net/publication/6676597>

An Evaluation of DGT Performance Using a Dynamic Numerical Model

ARTICLE in ENVIRONMENTAL SCIENCE AND TECHNOLOGY · OCTOBER 2006

Impact Factor: 5.33 · DOI: 10.1021/es061215x · Source: PubMed

CITATIONS

30

READS

25

4 AUTHORS:



Niklas Lehto

Lincoln University New Zealand

16 PUBLICATIONS **154** CITATIONS

[SEE PROFILE](#)



William Davison

Lancaster University

237 PUBLICATIONS **10,055** CITATIONS

[SEE PROFILE](#)



Hao Zhang

Lancaster University

191 PUBLICATIONS **6,704** CITATIONS

[SEE PROFILE](#)



Wlodek Tych

Lancaster University

95 PUBLICATIONS **1,698** CITATIONS

[SEE PROFILE](#)

An Evaluation of DGT Performance Using a Dynamic Numerical Model

NIKLAS J. LEHTO, WILLIAM DAVISON,*
HAO ZHANG, AND WŁODEK TYCH

*Environmental Science Department, Lancaster University,
Bailrigg, Lancaster, LA1 4YQ, United Kingdom.*

A numerical model of the transport and dynamics of metal complexes in the resin and gel layers of a DGT (diffusive gradients in thin films) device was developed and used to investigate how the chelating resin and metal–ligand complexes in solution affect metal uptake. Decreasing the stability constant or concentration of the binding resin increases the competition for free metal ions by ligands in solution, lowering the rate of mass uptake. Such effects would be rarely observed for moderately or strongly binding resins ($K > 10^{12}$), including Chelex, which out-compete labile ligands in solution. With weakly binding resins, strongly bound solution complexes can diffuse into the resin layer before a measurable amount of dissociation occurs, such that concentrations of bound metal at the rear and front surfaces of the resin layer are equal. With more strongly binding resins, metal mainly binds to the front surface of the resin. Only complexes with the largest binding constants penetrate the gel layer containing Chelex, but their lack of lability means that the DGT sensitivity to the complex is, in any case, very low. The slow diffusion of complexes, such as those of fulvic acids, which increases the time required to establish steady state, compromises the use of the simple DGT equation. Errors are negligible for 24 h deployments, when diffusive layer thicknesses are less than 1 mm, but 3 day deployments are required to ensure accuracy with 2.4 mm thick layers. The extent to which the commonly used equation, that accounts for the concentration and diffusion of metal–complex species, overestimates DGT uptake if the rate of dissociation is slow, was estimated.

Introduction

It is generally accepted that the toxicity of many metals in aquatic environments is related to the activity of the free metal ion (1). This has given rise to the free ion activity model (FIAM) (2) and, more recently, the biotic ligand model (BLM) (3), which have successfully predicted metal toxicities in simple solutions containing well-defined ligands (4). However, the free metal ion is not always the best predictor of total bioavailability (5, 6). Uptake of the free ion at a biological membrane can perturb the equilibrium with other metal species and cause dissociation of metal complexes. In cases where there is rapid biological uptake, the diffusional supply of metal complexes and their kinetics of dissociation can limit the availability of the free metal ion. Assessment of total metal bioavailability then requires information on the proportional amounts, and rates of dissociation, of various metal species.

Diffusive gradients in thin films (DGT) (7) has been established as a robust in situ method for investigating metal speciation in natural systems. This dynamic technique can also provide information on the kinetics of complex dissociation in aquatic systems (8, 9) and of release from solid phase in soils and sediments (10, 11).

The DGT device contains a binding phase, which is often a layer of Chelex-100 resin embedded in a hydrogel. This resin–gel layer is separated from the bulk solution by a well-defined diffusive layer of gel (the diffusive gel), the thickness of which can be varied. The resin selectively binds metal ions that diffuse from the bulk solution, through the diffusive layer and into the resin–gel. Because the metal is continually removed from the gel-entrained solution, a constant diffusive gradient is quickly established through the diffusive gel and maintained by convective supply in solution. The total amount of metal accumulated is determined by the amount of metal available to the resin during the deployment of the device. This is controlled by the following:

- (1) the thickness of the diffusive layer, which determines the length of the diffusive pathway between the resin and the bulk solution;
- (2) the diffusive properties of the free metal ion, free ligand and the metal–ligand complex;
- (3) the concentration of free metal in the bulk solution;
- (4) the concentration of complexed metal in the bulk solution and its dissociation rate.

When DGT is deployed under well stirred conditions, such that there is a negligible diffusive boundary layer at the surface of the device, and there is no significant depletion of free metal ion in the bulk solution, there is net dissociation of the complex in the diffusive and resin gel layers. The net dissociation of the dynamically exchanging complex occurs as re-formation of the complex is prevented by the sequestration of the dissociated metal (resin layer) and consequent imposition of a diffusive gradient (diffusive layer).

Models have been constructed to describe the behavior of the free metal, -ligand, and metal–ligand complexes of different stabilities in the diffusive layer (8, 12) and in both the diffusive and resin–gel layers (13). An underlying assumption of the models has been that free metal is instantaneously and irreversibly removed by the binding phase, resulting in a negligible concentration in the resin layer. These models have been validated experimentally by DGT deployments in a range of simple solutions where three principal species have been considered: free metal ion (Cu and Ni), free ligand (citrate, NTA, EDTA, fulvic acid (FA), and humic acid (HA)) and metal–ligand complex (13, 14). The removal of the free ion prevents the reformation of metal complexes resulting in net dissociation. Hence DGT measures the free metal ion plus labile species, which are defined as those complexes that can dissociate within a time determined by the diffusion layer thickness and the diffusion coefficient of the complex.

Various methods using Chelex-100 and other resins have been used to determine the proportion of complexed metal and dissociation rate constants of complexes in natural waters (15–18). In situ DGT measurements of Cd and Cu (19) and Hg (20) suggest that DGT-measured labile metal fractions measured with different binding phases can be significantly different, implying that the proportion of complexes detected as labile is influenced by the binding strength of the binding phase used in DGT devices. This effect cannot be explored using the previously described models of DGT where the binding phase is simply described as a sink for free metal ions. We have developed a new dynamic DGT uptake model

* Corresponding author phone: + 44 1524 593935; fax: + 44 1524 593985; e-mail: w.davison@lancaster.ac.uk.

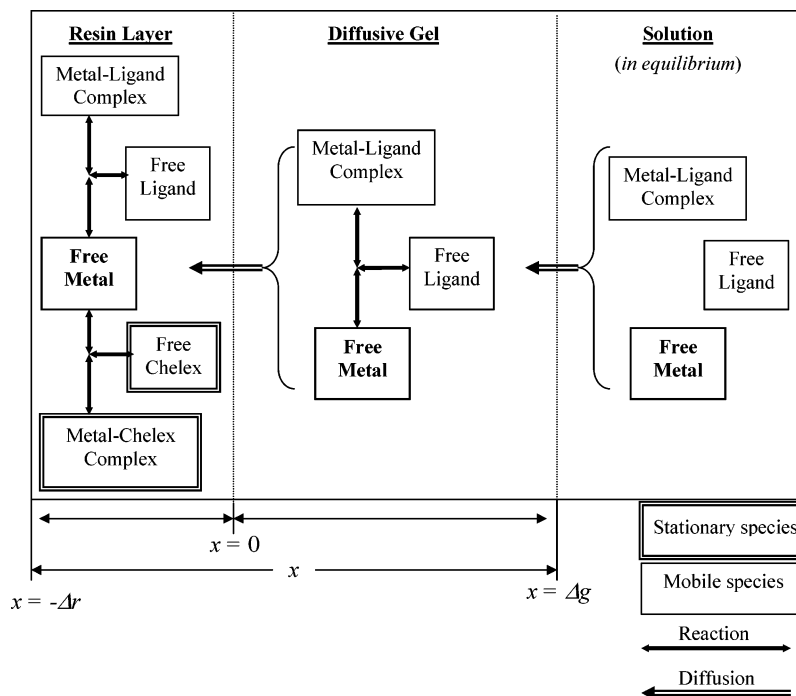


FIGURE 1. Schematic illustration of the concepts of the numerical model.

where the resin in the resin-layer is defined as an immobilized ligand, as described by Chakrabarti et al. (15). The concentrations of the binding sites and their formation and dissociation rate constants are modified to explore the effect that the use of different types and quantities of binding resins can have on DGT measurements in solutions of metal ions and metal–ligand complexes. The model predictions are used to demonstrate the importance of both thermodynamic (stability constants) and kinetic (rate constants) controls on the DGT measurement and to assess the accuracy of previous interpretations of speciation measurements in natural waters using DGT.

Model Concepts and Formulation

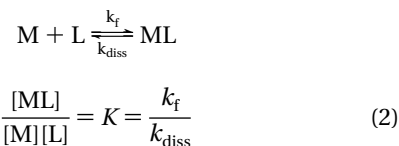
Basic concepts of transport and reaction (Figure 1) used by the dynamic model are discussed prior to giving its mathematical formulation. Transport of mobile species in the diffusive layer and the resin layer is assumed to occur solely by molecular diffusion according to Fick's Law. The concentration of the species is determined by the diffusion of the species and any reactions, R_E , that may affect it (eq 1).

$$\frac{\partial C}{\partial t} = D_{s,m} \frac{\partial^2 C}{\partial x^2} + R_E \quad (1)$$

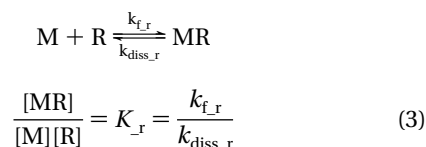
$D_{s,m}$ is the diffusion coefficient of species “s” in medium “m”, as individual diffusion coefficients depend on the species, the medium, and the temperature.

Metal exists in one of three separately modeled species: a mobile free metal species (M), a mobile metal–ligand complex (ML), and an immobile metal–resin species (MR). There is additionally the mobile free ligand (L) and the immobile resin (R). The exchange reactions between the free metal and the ligand, and the free metal and the resin, obey first order kinetics and 1:1 complexes are assumed to form preferentially. Consequently, within the resin layer, binding sites, and the free ligand compete for the free metal. The time taken to reach steady state is dependent upon the diffusion coefficients of the species and their rates of dissociation in the resin and diffusive layers.

The equilibrium relationships between the concentrations of different species ([M], [L], [ML], and [MR]) are expressed by eqs 2 and 3.



and



Where k_f (metal–ligand) and k_{f_r} (metal–resin) ($\text{mol L}^{-1} \text{s}^{-1}$) are the complex formation rate constants; k_{diss} (metal–ligand) and k_{diss_r} (metal–resin) (s^{-1}) are the complex dissociation rate constants; K (metal–ligand) and K_{resin} (metal–resin) (mol L^{-1}) are the complex stability constants. The effect of different metal–ligand complexes and binding phases on DGT uptake can be simulated by modifying the formation and dissociation rate constants.

The resin species are considered to be stationary in the resin gel ($-\Delta r \leq x \leq 0$; Figure 1). The free metal and the ligand species are mobile in the resin and diffusive gels ($-\Delta \leq x \leq \Delta g$). The reaction and transport of the different species are described by eqs 4–11 in Table 1. For mobile species, the first part of the equation represents the first-order kinetics of exchange between the free metal (M), ligand (L) and the metal–ligand complex (ML). The second part of the equation describes the diffusion of each species in terms of its concentration and diffusion coefficient. Although the metal bound to the resin may have some mobility, enabling it to migrate slowly between resin binding sites, this is unlikely to have an effect in the time periods simulated in this work

TABLE 1. Equations That Describe the Behavior of Metal, Ligand and Complex in the Diffusive Gel and the Resin Gel

species	domain	equation	eq. no.
free metal in diffusive gel	$(0 < x < \Delta g)$	$\frac{\partial [M_x]}{\partial t} = k_{\text{dis}}[ML_x] - k_f[M_x][L_x] + \frac{\partial}{\partial x} \left(D_{M-g} \frac{\partial [M_x]}{\partial x} \right)$	4
free ligand in diffusive gel	$(0 < x < \Delta g)$	$\frac{\partial [L_x]}{\partial t} = k_{\text{dis}}[ML_x] - k_f[M_x][L_x] + \frac{\partial}{\partial x} \left(D_{L-g} \frac{\partial [L_x]}{\partial x} \right)$	5
metal–ligand complex in diffusive gel	$(0 < x < \Delta g)$	$\frac{\partial [ML_x]}{\partial t} = k_f[M_x][L_x] - k_{\text{dis}}[ML_x] + \frac{\partial}{\partial x} \left(D_{ML-g} \frac{\partial [ML_x]}{\partial x} \right)$	6
free metal in resin gel	$(-\Delta r < x \leq 0)$	$\frac{\partial [M_x]}{\partial t} = k_{\text{dis}_r}[MR_x] - k_{f_r}[M_x][R_x] + k_{\text{dis}}[ML_x] - k_f[M_x][L_x] + \frac{\partial}{\partial x} \left(D_{M-r} \frac{\partial [M_x]}{\partial x} \right)$	7
free ligand in resin gel	$(-\Delta r < x \leq 0)$	$\frac{\partial [L_x]}{\partial t} = k_{\text{dis}}[ML_x] - k_f[M_x][L_x] + \frac{\partial}{\partial x} \left(D_{L-r} \frac{\partial [L_x]}{\partial x} \right)$	8
metal–ligand complex in resin gel	$(-\Delta r < x \leq 0)$	$\frac{\partial [ML_x]}{\partial t} = k_f[M_x][L_x] - k_{\text{dis}}[ML_x] + \frac{\partial}{\partial x} \left(D_{ML-r} \frac{\partial [ML_x]}{\partial x} \right)$	9
free Chelex in resin gel	$(-\Delta r < x \leq 0)$	$\frac{\partial [R_x]}{\partial t} = k_{\text{dis}_r}[MR_x] - k_{f_r}[M_x][R_x]$	10
metal–Chelex complex in resin gel	$(-\Delta r < x \leq 0)$	$\frac{\partial [MR_x]}{\partial t} = k_{f_r}[M_x][R_x] - k_{\text{dis}_r}[MR_x]$	11

TABLE 2. Model Input for Analyzing the Effect of the Resin Stability Constant on Metal Uptake in the Presence of Different Ligands

	diffusion coefficients		rate constants		stability constants	reactant concentrations			
	diffusive gel $D_M = D_L = D_{ML}$ (cm ² s ⁻¹)	resin gel $D_M = D_L = D_{ML}$ cm ² s ⁻¹)	k_f (L s ⁻¹ mol ⁻¹)	k_{diss} (s ⁻¹)	K_{eq} L mol ⁻¹	[metal] (mol L ⁻¹)	[ligand] (mol L ⁻¹)	[metal–Ligand] (mol L ⁻¹)	Σ metal (mol L ⁻¹)
ligand 1	5×10^{-6}	5×10^{-6}	1×10^9	1×10^3	10^6	1.01×10^{-7}	1.00×10^{-7}	1.01×10^{-11}	1.01×10^{-7}
ligand 2	5×10^{-6}	5×10^{-6}	1×10^9	1×10^1	10^8	1.00×10^{-7}	1.00×10^{-7}	1.00×10^{-9}	1.01×10^{-7}
ligand 3	5×10^{-6}	5×10^{-6}	1×10^9	1×10^{-2}	10^{11}	9.18×10^{-9}	1.00×10^{-7}	9.18×10^{-8}	1.01×10^{-7}
ligand 4	5×10^{-6}	5×10^{-6}	1×10^9	1×10^{-3}	10^{12}	1.00×10^{-9}	1.00×10^{-7}	1.00×10^{-7}	1.01×10^{-7}
ligand 5	5×10^{-6}	5×10^{-6}	1×10^9	1×10^{-4}	10^{13}	1.01×10^{-10}	1.00×10^{-7}	1.01×10^{-7}	1.01×10^{-7}
ligand 6	5×10^{-6}	5×10^{-6}	1×10^9	1×10^{-5}	10^{14}	1.01×10^{-11}	1.00×10^{-7}	1.01×10^{-7}	1.01×10^{-7}

The initial and boundary conditions for the domain are described in the Supporting Information (Table S1). At the interface of the resin gel and the diffusive gel ($x = 0$) an interfacial condition is implemented to ensure equal fluxes and concentration continuity of each species on both sides of the boundary, consistent with there being no changes in solubility or Donnan potential between the two phases.

If the diffusive gel or filter has an inherent charge, a discontinuity in concentration can occur at the boundary between them or with the bulk solution, due to the formation of a Donnan potential (21, 22). However, the potential is negligible for gels commonly used for DGT when deployment solutions have ionic strengths $\geq 1 \text{ mmol L}^{-1}$ (23). Therefore, such effects have not been considered in this work.

Model Solution. Due to the nonlinearity of the continuity eqs (4–11), a numerical solution is required. The finite element method (FEM) was used to solve the systems of nonlinear PDEs by applying the FEMLAB package supplied by COMSOL, UK. FEMLAB applies dynamic unstructured adaptive-grid methods to optimize the numerical solution. The total number of elements varies depending on the size of the diffusive and resin layers considered and on the accuracy required. At the resin–gel/diffusive–gel interface the spatial resolution of the calculations was 10^{-7} cm and the temporal resolution varied from 0.001 to 10s. With the input parameters listed in Table 2 the model can be used to calculate the concentrations of all five species at any time

and point within the model domain. The total amount of metal taken up by the resin layer is calculated by integrating the total mass of metal–resin complex formed at $-\Delta r \leq x \leq 0$ over the simulated deployment time.

Results and Discussion

The Effect of the Stability of the Resin–Metal Complex and the Binding Site Concentration on Metal Uptake. When systems approach equilibrium, it is possible to discriminate between metal in different metal–ligand species using a range of different binding resins (16). The influence of these thermodynamic controls on the DGT measurement, where the flux is primarily controlled by a diffusion gradient, is explored here by considering resins with a range of binding strengths.

The thickness of the resin layer was taken to be 0.025 cm, as commonly used in DGT experiments. Binding sites were considered to be homogeneously distributed through the layer, with a concentration of either 0.1 mol L^{-1} , which is consistent with the amount of Chelex-100 resin used in a standard DGT device, or 1 mmol L^{-1} to represent an extreme case of low capacity. Garmon et al. (9) reported that Chelex resin beads are concentrated at one side of the resin layer due to the settling of the beads during casting of the resin gel, but with smaller bead size resins, the beads have been found to be homogeneously distributed (24). The rate

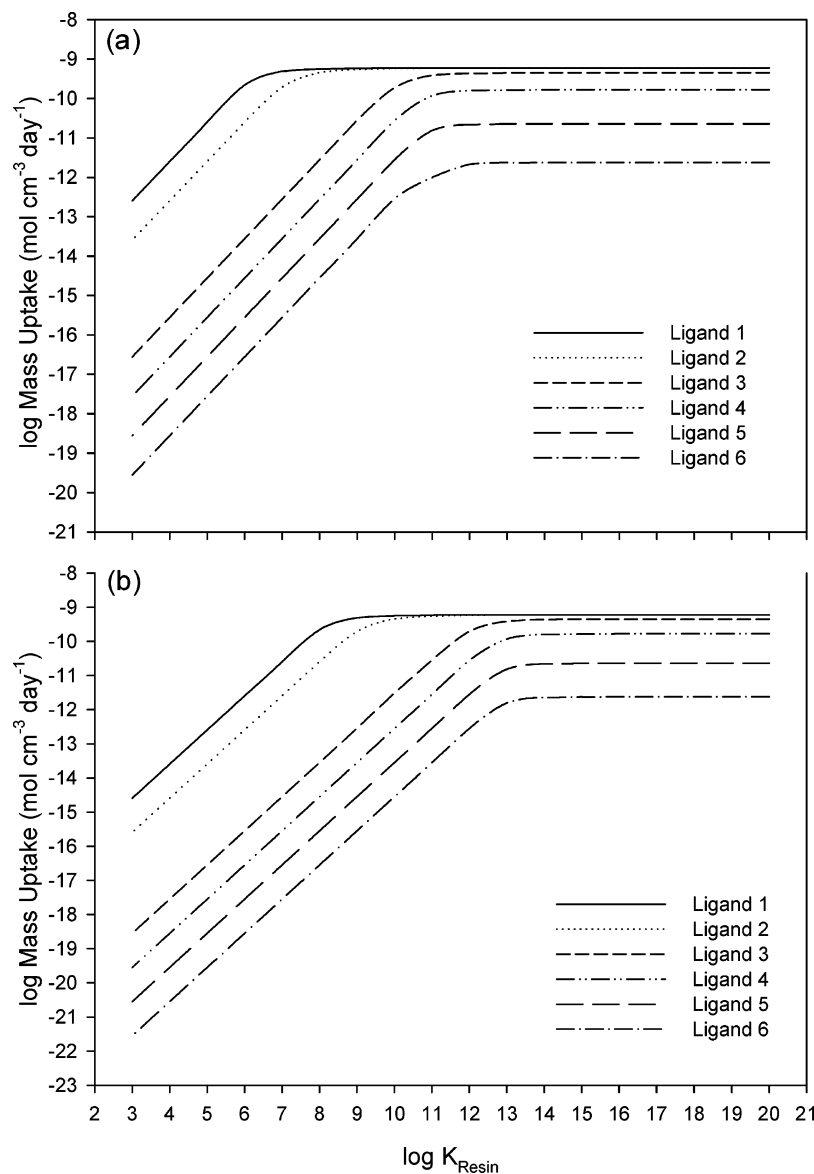


FIGURE 2. The effect of modifying the stability constant of the binding phase on DGT uptake of metal in the presence of ligands that form complexes of varying lability (Table 2). Two different resin binding site concentrations are simulated: 0.1 mol L⁻¹ (a) and 1 mol L⁻¹ (b). The following parameters were used in the modeling: Δg , 0.08 cm; [L], 10⁷ mol L⁻¹; t , 24 h; $D_M = D_L = D_{ML} = 5 \times 10^{-6}$ cm² s⁻¹.

constant for metal association with the resin was set at a value of 10⁹ L s⁻¹ mol⁻¹, which is representative of fast water loss, as observed for the Eigen mechanism (25). A range of dissociation rate constants were considered, with the highest value of 10⁻¹¹ s⁻¹ ($\log K_{\text{resin}} = 20$) being representative of a very stable metal-resin complex and the lowest value of 10⁵ s⁻¹ ($\log K_{\text{resin}} = 4$) representing a weak binding phase. The binding constant for metal–Chelex complexes is similar to that for metal EDTA complexes ($\log K_{\text{resin}} = 18$ for Cd) (26).

The effect of six hypothetical ligands (Table 2) on metal uptake by DGT in a 24 h period was modeled while varying the stability constant of the metal-resin complex, K_{resin} . The stability constant of metals with the solution ligands, K , was varied from 10⁶ to 10¹⁴ L mol⁻¹ to represent a range of dissociation rates encompassing very labile to virtually inert conditions. Changing K had an effect on the equilibrium concentrations of the different species. As the focus of the work was the effect of the immobilized binding agent, the binding in solution, represented by the ligand concentration, was kept constant, while the metal and metal–ligand complex concentrations were adjusted appropriately to maintain

equilibrium. The total concentration of metal species in the system was kept constant.

Decreasing $\log K_{\text{resin}}$ from 20 to 12 (Figure 2a) had no effect on the metal uptake by the binding phase. However, changing the dissociation rate of the complex in solution by changing its binding constant (ligands 1–6, Table 2) had a large effect on the DGT uptake (Figure 2a). The accumulated mass of metal is more affected by K_{resin} for systems with more strongly binding ligands in solution. As $\log K_{\text{resin}}$ is decreased to <12, the amount of metal-resin complex formed decreases, especially for the systems with the most stable ligands (ligands 5 and 6), due to increased competition for the free metal ion by the ligand.

Decreasing the concentration of the resin binding sites by 2 orders of magnitude had little effect on the mass taken up over the 24 h for binding resins with very large stability constants ($\log K \geq 14$) (Figure 2b). However, the threshold binding constant where competitive effects with the ligand in solution are observed is higher when the concentration of binding sites is 1 mmol L⁻¹. Uptake decreases for systems, with ligands 5 and 6, which have resin stability constants

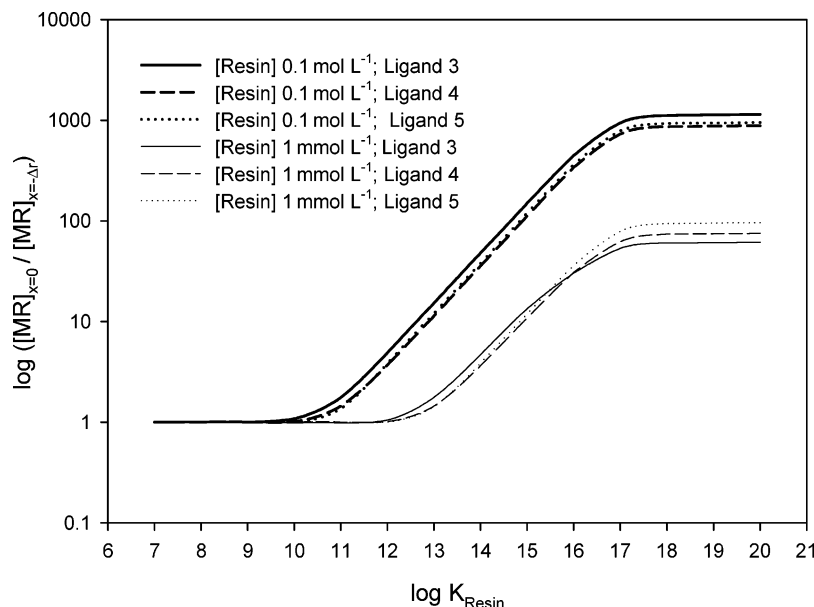


FIGURE 3. The effect of metal–ligand complex lability and the stability constant and concentration of binding sites in the resin phase on the distribution of metal–resin complex formed in the resin layer during a 24 h deployment. The ratio of metal–resin complex concentration at $x = 0$ to the concentration at $x = -\Delta r$ is shown to be influenced by the amount of resin binding sites present, the stability constant of the resin, and the stability constant of the metal–ligand complex. The initial metal, ligand, and complex concentrations and their diffusion coefficients used in these simulations are listed in Table 2.

less than $10^{14} \text{ L mol}^{-1}$. This is consistent with eq 7 (Table 1): as the concentration of the resin decreases it competes less effectively for the free metal, so more metal is retained by the metal–ligand complex.

The use of different types and quantities of resins in DGT devices presents interesting possibilities for the use of the technique in characterizing species distributions in natural systems.

The Effect of Metal Complexation on Metal–Resin Concentration Profiles Inside the Resin-Layer. The model allows the calculation of the spatial and temporal distribution of the concentration of species within the DGT device. Previous experiments showed that increasing the thickness of the resin layer, by using multiple resin layers, can result in a greater mass of metal taken up by DGT (9), especially when a relatively stable metal–ligand complex is present in solution. Figure 3 shows the ratio of the concentration of the metal–resin complex formed at the interface of the resin-gel ($x = 0$) and the diffusive gel to the amount of complex formed at the part of the resin gel farthest away from the diffusive gel ($x = -\Delta r$). This ratio provides an indication of where in the DGT device free metal is sequestered by the resin due to the net rate of dissociation being sufficient to increase the free metal ion concentration over its value at equilibrium, as determined by the concentrations of the resin binding sites and resin–metal complex ($[R]$ and $[MR]$ respectively), and the stability constant of the resin (K_{resin}). A high ratio is indicative of a DGT-labile complex, which has dissociated either prior to diffusing into the resin layer or immediately upon entering it. A low ratio (around 1) is indicative of a more inert complex that has diffused into the resin layer and is undergoing net dissociation progressively within it. This ratio was calculated for a variety of ligand and resin binding strengths at two concentrations of resin binding sites, with examples shown in Figure 3. In the presence of the most labile complexes, the ratio was in the region of 10^{13} (not shown), indicating that metal is bound immediately; it contacts the resin, with negligible penetration into the resin-layer, provided there are no capacity issues. This finding further justifies the use of the simple DGT equation for calculating the accumulated mass per unit area, M_a , proposed

by Davison and Zhang (7) (eq 12), where c_{metal} is the concentration in the bulk solution.

$$M_a = \frac{c_{\text{metal}} \times D_{\text{metal}} \times t}{\Delta g} \quad (12)$$

The diffusion coefficient of metal in the diffusive layer, of thickness Δg , is D_{metal} , and t is the deployment time. As the lability of metal–ligand complexes is progressively decreased (smaller k_{diss}), the ratio at $[R] = 0.1 \text{ mol L}^{-1}$ decreases due to the complexes penetrating further into the resin layer. At $[R] = 1 \text{ mmol L}^{-1}$, the ratio increases because the relative stability of the complex limits its dissociation within the resin layer. Reducing the stability or concentration of binding sites also lowers the ratio, as it reduces the resin layer's competitiveness for the free metal and the complex is able to diffuse further into the resin layer before it is bound by the resin. With strongly binding Chelex ($\log K \sim 18$ for Cd) as the binding layer, at the high concentrations that it is generally used, there is negligible penetration of the complex for all but the strongest binding constants. However, the dissociation rate of such stable complexes is likely to be so small that there is little dissociation and consequently the sensitivity of the DGT method to metal in this complex is very low. In a natural water, with a range of ligand binding strengths, the effect of complex dissociation within the binding layer is, therefore, unlikely to be important.

Assessing the Reliability of the DGT Mass Uptake Equation. Equation 12 applies when a linear concentration gradient of metal from the bulk solution into the resin is established quickly and maintained throughout the deployment (steady-state flux) and the concentration of metal at the resin-diffusive layer interface is negligible (diffusion limiting conditions). Early calculations of DGT uptake were based on the situation in simple inorganic solutions, where all species contributing to the accumulated metal per unit area are fully labile and have effectively the same diffusion coefficient, allowing use of the simple eq 12 (7). These species can be referred to as dynamic, because they are both labile and mobile (27).

Use of eq 12 to calculate the mass uptake by the DGT resin requires the assumption that there is a constant flux

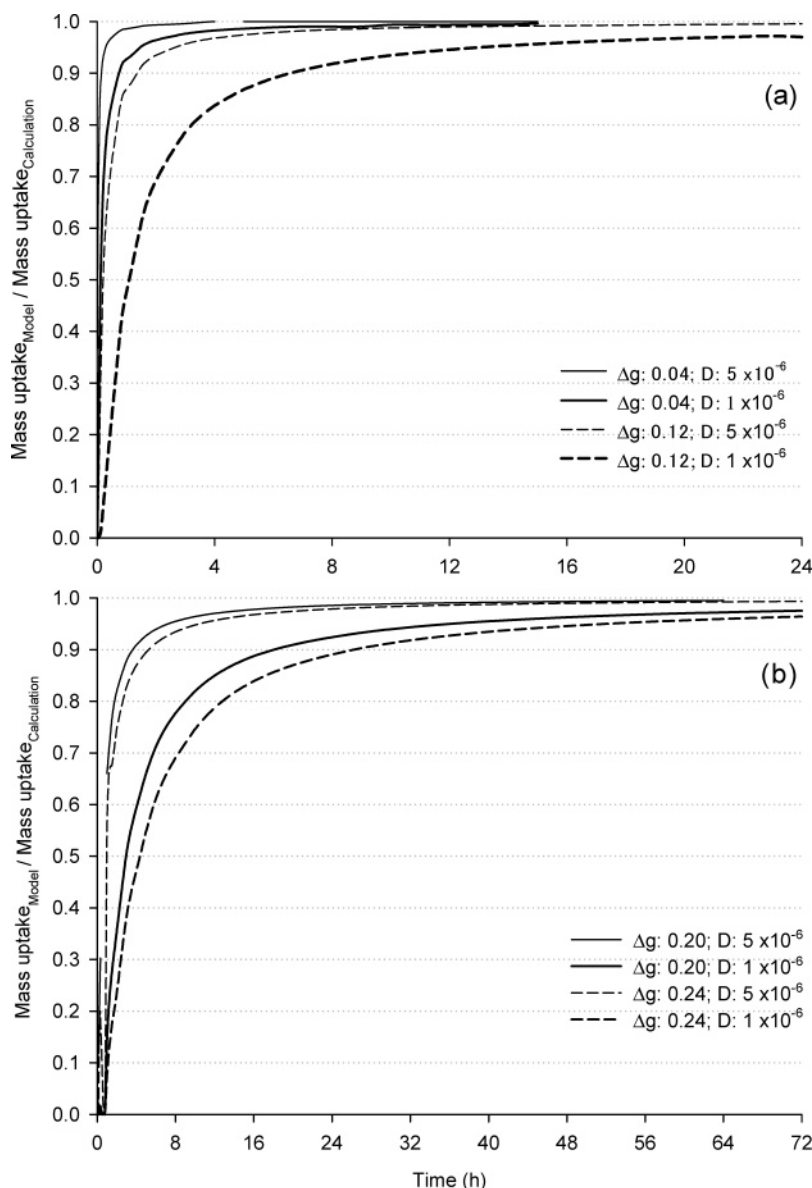


FIGURE 4. The ratio of calculated (eq 12) to modeled DGT mass uptake as a function of deployment time when the diffusion coefficient (D) is modified from 1×10^{-6} to 5×10^{-6} cm² s⁻¹ and the gel layer thickness (Δg) is varied between 0.04 and 0.12 cm (a); 0.2 and 0.24 cm (b).

of metal into the resin throughout the deployment of the device. This is not the case, as discussed in some detail by van Leeuwen (28). In the early stages of the deployment, before steady state is reached, the flux is lower. The time required to reach steady-state depends, among others, on the diffusion coefficient of the metal and the thickness of the diffusion layer. The extent to which eq 12 overestimates the total mass accumulated by the DGT device depends on the total deployment time. As no steady state assumptions are made in using the dynamic model, it can be used to investigate the error incurred in using eq 12. Figure 4 shows how the ratio of modeled mass uptake to calculated mass uptake (eq 12) changes with different deployment times. Two diffusion coefficients, typical of inorganic complexes (5×10^{-6} cm² s⁻¹) and fulvic acid complexes (1×10^{-6} cm² s⁻¹) are considered for a range of commonly used gel layer thicknesses: (a) 0.04 and 0.12 (b) 0.20 and 0.24. Even for the thickest gels errors are within the usual precision of DGT measurements ($\pm 5\%$) for deployments exceeding 10 h in simple inorganic solutions, while for the commonly used 0.04 and 0.08 cm gel layer thicknesses there are only minimal errors for 4 h deployments. For fulvic acid complexes,

measurements are accurate for the thinner gels with 24 h deployments, but deployments of up to 3 days are required for the thickest gels to ensure accurate calculation of the results.

Interpretation of data from in situ deployments in natural systems requires a different approach as metal is usually present in various complex forms. To be able to calculate the mass of metal accumulated by DGT in natural systems accurately, the concentrations and diffusion coefficients of the ligands and the metal–ligand complexes need to be considered (29). Several workers have done this by using variations of eq 13, which is based on the assumption that metal–ligand complexes dissociate completely either just before or at the binding layer and can be represented by a single concentration and diffusion coefficient (29–31). Contributions to the total accumulated mass per unit area are simply obtained by adding the two terms based on eq 12. At steady state the equilibrium between complex and metal is preserved by their linear concentration gradients, such that D_{metal} and D_{complex} can be used independently (14, 32). The major shortcoming of this approach is that it fails

$$M_a = \left(\frac{c_{\text{metal}} \times D_{\text{metal}} \times t}{\Delta g} \right) + \left(\frac{c_{\text{complex}} \times D_{\text{complex}} \times t}{\Delta g} \right) \quad (13)$$

to consider the dissociation kinetics of the metal–ligand complex.

The numerical model, which considers the kinetic-limited dissociation of the complex at all locations and automatically accounts for differences in the diffusion coefficients of metal and complex, was used to assess the accuracy with which eq 13 can predict DGT metal uptake for three different metals: cobalt, zinc, and cadmium in the presence of a high ligand concentration (1 mmol L⁻¹). Table 3a shows the distribution of metal between two species, (uncomplexed) metal and the metal complex. To facilitate easy comparison between the metals, the same set of complex stability constants were used and dissociation rate constants (k_{diss}) were adjusted accordingly. Substitution of the concentration of the two species in eq 13 allows calculation of the mass uptake by a DGT device for a certain deployment time and diffusion layer thickness for a range of cases where the diffusion coefficient of the complex is modified. The diffusion coefficient of the metal, D_M , was set at 5×10^{-6} cm² s⁻¹ and the diffusion coefficient of the complex, D_{ML} was varied so that D_{ML}/D_M was in the range 0.1–1. In the model simulations the diffusion coefficient of the ligand was assumed to be the same as that of the complex. Metal uptake was also calculated using the model, where the kinetics of complex dissociation are taken into account. Table 3b shows how the ratio, R_{AM} , of the model-predicted accumulated mass to the equation-predicted accumulated mass, depends on the (metal specific) formation rate constant, the diffusion coefficient of the complex and its stability constant (as specified by the dissociation rate constant, which is specific to the ligand). A ratio of 1 indicates that the equation predicts the contribution of the complex-

bound metal accurately and that uptake is only limited by the diffusion of the metal and the complex. As the ratio approaches 0 the kinetics increasingly limit the total metal uptake.

Table 3b can be divided into two parts, shown by a more solid line, according to the agreement between eq 13 and model predictions for the $D_{ML} = D_M$ case. Values of R_{AM} are nearest 1 to the left of the line because a substantial proportion of metal is uncomplexed and the dissociation rate constant is relatively high. The line moves progressively to higher K values for Zn and Cd because of the order of increasing dissociation rate constants (Cd > Zn > Ni). Immediately to the left or right of the solid line R_{AM} has a value of 1.00 or 0.99 when $D_M = D_{ML}$, indicating that kinetic limitation is negligible. The slight decrease in R_{AM} as D_{ML}/D_M decreases is due to the slow diffusion of the complex slowing the approach to steady state. Calculation of the concentration profiles of individual species through the device shows that the free metal has almost reached steady state after 24 h (Supporting Information: Figure S1a). Initially the free metal concentration is effectively buffered by the dissociating complex (the first 20 min of the simulation). The concentration profile of the complex shows that the complex has completely dissociated, either by the time it reaches the resin or immediately after, whereas the ligand progressively accumulates in the resin gel. At substantially higher values of $\log K$, R_{AM} is much lower, but it increases as D_{ML}/D_M decreases, in line with previous predictions of complex lability (13). This effect is more pronounced at higher values of $\log K$. When $D_{ML}/D_M = 1$ there is severe kinetic limitation at $\log K = 11$ for Co, but this limitation is much less pronounced as D_{ML}/D_M decreases, consistent with the increasing residence time of complex in the diffusion layer due to a smaller value of D_{ML} .

TABLE 3. (a) The Formation (k_f) Rate Constants of Co, Zn, and Cd (based on Morel and Hering (25), Assuming an Ionic Strength of 0.002 mol L⁻¹) and Associated Dissociation Rate Constants (k_{diss}) for a Range of Stability Constants and Solution Compositions. (b) The Effect of Metal Formation Rate Constant (k_f), Stability Constant, and Diffusion Coefficient of the Complex ($D_{ML} = D_L$), on the Ratio of Metal Uptake Calculated by the Model to the Uptake Calculated by eq 13 for a 24 h Deployment When the Total Metal Concentration (free Metal + Ligand-Bound Metal) is Maintained Constant at 1.01×10^{-7} mol L⁻¹.^a

cobalt			zinc			cadmium			[metal] mol L ⁻¹	[ligand] mol L ⁻¹	[metal– ligand] mol L ⁻¹	Σ metal mol L ⁻¹
k_f L s ⁻¹ mol ⁻¹	k_{diss} s ⁻¹		k_f L s ⁻¹ mol ⁻¹	k_{diss} s ⁻¹		k_f L s ⁻¹ mol ⁻¹	k_{diss} s ⁻¹					
1.32×10^6	1.32×10^3		4.62×10^4			1.98×10^5			5.05×10^{-8}		5.05×10^{-8}	1.01×10^{-7}
	1.32×10^1		4.62×10^2			1.98×10^3			1×10^{-9}		1.00×10^{-7}	1.01×10^{-7}
	1.32		4.62×10^1			1.98×10^2			1.01×10^{-10}		1.01×10^{-7}	1.01×10^{-7}
	1.32×10^{-1}	4.62×10^7	4.62		1.98×10^8	1.98×10^1			1.01×10^{-11}	10^{-3}	1.01×10^{-7}	1.01×10^{-7}
	1.32×10^{-2}		4.62×10^{-1}			1.98			1.01×10^{-12}		1.01×10^{-7}	1.01×10^{-7}
	1.32×10^{-3}		4.62×10^{-2}			1.98×10^{-1}			1.01×10^{-13}		1.01×10^{-7}	1.01×10^{-7}
	1.32×10^{-4}		4.62×10^{-3}			1.98×10^{-2}			1.01×10^{-14}		1.01×10^{-7}	1.01×10^{-7}
	1.32×10^{-5}		4.62×10^{-4}			1.98×10^{-3}			1.01×10^{-15}		1.01×10^{-7}	1.01×10^{-7}
b												
	D_{ML}/D_M	$\log K_{\text{eq}} 3$	$\log K_{\text{eq}} 5$	$\log K_{\text{eq}} 6$	$\log K_{\text{eq}} 7$	$\log K_{\text{eq}} 8$	$\log K_{\text{eq}} 9$	$\log K_{\text{eq}} 10$	$\log K_{\text{eq}} 11$			
cobalt	1.0	1.00	1.00	0.99	0.97	0.91	0.71	0.24	0.03			
	0.5	1.00	0.99	0.99	0.98	0.93	0.80	0.38	0.06			
	0.2	1.00	0.99	0.98	0.98	0.95	0.86	0.59	0.14			
	0.1	1.00	0.98 ^b	0.97	0.97	0.95	0.94	0.89	0.24			
zinc	1.0	1.00	1.00	1.00	0.99	0.98	0.95	0.85	0.51			
	0.5	1.00	1.00	0.99	0.99	0.98	0.96	0.89	0.65			
	0.2	1.00	0.99	0.99	0.99	0.98	0.97	0.92	0.78			
	0.1	1.00	0.98	0.98	0.97	0.96						
cadmium	1.0	1.00	1.00	1.00	0.99	0.99	0.97	0.93	0.77			
	0.5	1.00	1.00	1.00	0.99	0.99	0.98	0.94	0.82			
	0.2	1.00	0.99	0.99	0.99							
	0.1	1.00	0.98	0.98	0.99							

^a A 0.08 cm thick diffusion layer was used. Results are not available for cases involving slow diffusing and very slowly dissociating Cd and Zn complexes ($\log K \geq 8$) due to numerical limitations arising from very stiff equations. $\log K$ for the metal–resin complex was 18. ^b Figure S1a.

Model simulations were used to assess the effect of the ligand concentration on cobalt uptake, with other conditions being those adopted for Table 3 (Supporting Information Table 2a and b). When the concentration of the ligand is low (10^{-7} M), a relatively high value of $\log K$ of 8 is required before the complex dominates the solution composition. For $\log K \geq 9$, the effect of kinetic limitation, as measured by R_{AM} , is virtually independent of the ligand concentration and dependent solely on K and hence k_{dis} . The concentration profiles of individual species through the device for an example kinetically limited case ($[L] = 10^{-7}$ mol L $^{-1}$, $\log K = 8$, $D_{ML}/D_M = 1$) show that penetration of the complex into the resin layer lowers the steady-state concentration gradient and consequently the flux (Supporting Information, Figure S1b).

Fulvic acids are the major binding ligands in most fresh waters. The diffusion coefficients of their metal complexes in the diffusive layer are typically 20% of the diffusion coefficients of the free metal ion ($D_{ML}/D_M = 0.2$) (30). Average log stability constants for metal complexes with the stronger phenolic sites can be estimated from the default binding parameters used for the WHAM speciation model (33): Cd and Zn, 5.65; Pb, 7.68; Cu 7.34; etc. The total concentration of these binding sites for a water containing 4 mg l $^{-1}$ of fulvic acid is typically 10^{-5} mol L $^{-1}$. Consideration of Table 3b and S2b suggests that for metals that have fast association rates, eq 13 should accurately predict the mass accumulated by DGT. For other metals with known kinetic limitations, such as Ni and possibly Co this may not be the case. Furthermore Cu is known to preferentially occupy the small number of binding sites that have constants substantially stronger than the mean phenolic site. The proportion of Cu occupying these sites may also be kinetically limited.

This work has shown the importance of both thermodynamic and kinetic factors in determining what is measured by DGT. To ensure that the primary step of sequestration of metal ions by the resin works efficiently for all solution conditions, the stability constant for the metal-resin interaction must be greater than a high threshold value. The metal exchange dynamics in solution then determines the extent of net dissociation of complexes, penetration of complexes into the resin layer, and consequently the proportion of metal that is measured.

Acknowledgments

This research has been jointly funded by The Natural Environment Research Council (UK) and the Macaulay Institute in Aberdeen, UK. We also acknowledge the constructive comments provided Øyvind Aaberg-Garmo and three anonymous reviewers.

Supporting Information Available

The boundary conditions used for the modeling, further comparisons of metal uptake calculated using the model and eq 13 and example time series of the distribution of species through the diffusive and resin layers. This material is available free of charge via the Internet at <http://pubs.acs.org>

Literature Cited

- (1) Tessier, A.; Buffle, J.; Campbell, P. G. C. In *Chemical and Biological Regulation of Aquatic Systems*; Buffle, J., DeVite, R. R. Eds.; Lewis Publishers: Boca Raton, FL, 1994; p 199.
- (2) Campbell, P. G. C.; Interactions between Trace Metals and Aquatic Organisms: A Critique of the Free-Ion Activity Model. In: *Metal Speciation and Bioavailability in Aquatic Systems*; Tessier, A., Turner, D. R., Eds.; Wiley: New York, 1995; pp 45–102.
- (3) Di Toro, D. M.; Allen, H. E.; Bergman, H. L.; Meyer, J. S.; Paquin, P. R.; Santore, R. C. Biotic Ligand Model of the Acute Toxicity of Metals. 1. Technical Basis. *Environ. Toxicol. Chem.* **2001**, *20*, 2383–2396.
- (4) DeSchampelaere, K. A. C.; Janssen, C. R. A biotic ligand model predicting acute copper toxicity to *Daphnia magna*: the effects of calcium, magnesium, sodium, potassium, and pH. *Environ. Sci. Technol.* **2002**, *36*, 48–54.
- (5) Hudson, R. J. M. Which aqueous species control the rates of trace metal uptake by aquatic biota? *Sci. Total. Environ.* **1998**, *219*, 95–115.
- (6) Mirimanoff, N.; Wilkinson, K. J. Regulation of Zn accumulation by a freshwater Gram-positive bacterium (*Rhodococcus opacus*). *Environ. Sci. Technol.* **2000**, *34*, 616–622.
- (7) Davison, W.; Zhang, H. In-situ speciation measurements of trace components in natural waters using thin-film gels. *Nature* **1994**, *367*, 546–548.
- (8) Scally, S.; Davison, W.; Zhang, H. In situ measurements of dissociation kinetics and labilities of metal complexes in solution using DGT. *Environ. Sci. Technol.* **2003**, *37*, 1645–1652.
- (9) Aaberg-Garmo, Ø.; Lehto, N.; Zhang, H.; Davison, W.; Røyset, O.; Steinnes, E. Effect of complexation on DGT sampling of lanthanoids in Multi-metal solutions. *Environ. Sci. Technol.* **2006**, in press.
- (10) Ernstberger, H.; Davison, W.; Zhang, H.; Tye, A.; Young, S. Measurement and dynamic modelling of trace metal mobilization in soils using DGT and DIFS. *Environ. Sci. Technol.* **2002**, *36*, 349–354.
- (11) Ernstberger, H.; Zhang, H.; Tye, A.; Young, S.; Davison, W. D. Desorption kinetics of Cd, Zn, and Ni measured in soils by DGT. *Environ. Sci. Technol.* **2005**, *39*, 1591–1597.
- (12) Salvador, J.; Puy, J.; Galceran, J.; Cecilia, J.; Town, R. M.; Van Leeuwen, H. P. Lability criteria for successive metal complexes in steady-state planar diffusion. *J. Phys. Chem. B* **2006**, *110* (2), 891–899.
- (13) Tusseau-Vuillemin, M.-H.; Gilbin, R.; Taillefert, M. A. A dynamic numerical model to characterize labile metal complexes collected with diffusive gradients in thin-films devices. *Environ. Sci. Technol.* **2003**, *37*, 1645–1652.
- (14) Zhang, H.; Davison, W. Direct in-situ measurements of labile inorganic and organically bound metal species in synthetic solutions and natural waters using diffusive gradients in thin-films. *Anal. Chem.* **2000**, *72*, 4447–4457.
- (15) Chakrabarti, C. L.; Lu, Y. Kinetic studies of metal speciation using chelex cation exchange resin: application to cadmium, copper, and lead speciation in river water and snow. *Environ. Sci. Technol.* **1994**, *28*, 1957–1967.
- (16) Pesavento, M.; Biesuz, R.; Alberti, G. Determination of the metal complexation capacity of natural waters by ligand titration in the presence of complexing resins. *J. Phys. IV France* **2003**, *107*, 1045–1048.
- (17) Apte, S. C.; Batley, G. E.; Bowles, K. C.; Brown, K. C.; Creighton, N.; Hales, L. T.; Hyne, R. T.; Julli, M.; Markich, S. J.; Pablo, F.; Rogers, N. J.; Stauber, J. L.; Wilde, K. A comparison of copper speciation measurements with the toxic responses of three sensitive freshwater organisms. *Environ. Chem.* **2005**, *2*, 320–330.
- (18) Bowles, K. C.; Apte, S. C.; Batley, G. E.; Hales, L. T.; Rogers, N. J. A rapid Chelex column method for the determination of metal speciation in natural waters. *Anal. chim. Acta* **2006**, *558*, 237–245.
- (19) Li, W.; Zhao, H.; Teasdale, P. R.; John, R.; Wang, F. Metal speciation measurements by diffusive gradients in thin films technique with different binding phases. *Anal. Chim. Acta* **2005**, *533*, 193–202.
- (20) Docekalova, H.; Divis, P. Application of diffusive gradient in thin films technique (DGT) to measurement of mercury in aquatic systems. *Talanta* **2005**, *65*, 1174–1178.
- (21) Fatin-Rouge, N.; Milon, A.; Buffle, J.; Tessier, A. Diffusion and partitioning of solutes in agarose hydrogels: The relative influence of electrostatic and specific interactions. *J. Phys. Chem. B* **2003**, *107*, 12126–12137.
- (22) Yezeck, L. P.; van Leeuwen, H. P. An electrokinetic characterization of low charge density cross-linked polyacrylamide gels. *J. Colloid Interface Sci.* **2004**, *278*, 243–250.
- (23) Warnken, K. W.; Zhang, H.; Davison, W. Trace metal measurements in low ionic strength synthetic solutions by diffusive gradients in thin films. *Anal. Chem.* **2005**, *77*, 5440–5446.
- (24) Warnken, K. W.; Zhang, H.; Davison, W. Performance characteristics of suspended particulate reagent – iminodiacetate as a binding agent for diffusive gradients in thin films. *Anal. Chim. Acta* **2004**, *508*, 41–51.
- (25) Morel, F. M. M.; Hering, J. G. *Principles and Applications of Aquatic Chemistry*; Wiley: New York, 1993.

- (26) Herrin, R. T.; Andren, A. W.; Armstrong, E. Determination of Silver Speciation in Natural Waters. 1. Laboratory Testes of Chelex-100 Chelating Resin as a Competing Ligand. *Env. Sci. Technol.* **2001**, 35 (10), 1953–1958.
- (27) Van Leeuwen H. P.; Town, R. M.; Buffle, J.; Cleven, R. F. M. J.; Davison, W.; Puy, J.; Van Riemsdijk, W. H.; Sigg, L. Dynamic speciation analysis and bioavailability of metals in aquatic systems. *Environ. Sci. Technol.* **2005**, 39, 8545–8556.
- (28) Van Leeuwen, H. P. Dynamic aspects of in situ speciation processes and techniques. In *In Situ Monitoring of Aquatic Systems: Chemical Analysis and Speciation*; IUPAC Series on Analytical and Physical Chemistry of Environmental Systems; Buffle, J., van Leeuwen, H. P., Eds.; Wiley: Chichester, 2000; Vol. 6, pp 253–277.
- (29) Unsworth, E. R.; Warnken, K. W.; Zhang, H.; Davison, W.; Black, F.; Buffle, J.; Cao, J.; Cleven, R.; Galceran, J.; Gunkel, P.; Kalis, E.; Kistler, D.; Van Leeuwen, H. P.; Michel, M.; Noel, S.; Nur, Y.; Odzak, N.; Puy, J.; VanRiemsdijk, W.; Sigg, L.; Temminghoff, W.; Tercier-Waeber, M.-L.; Toepperwien, S.; Town, R. M.; Weng, L.; Xue, H. Model predictions of metal speciation in freshwaters compared to measurements by in situ techniques. *Environ. Sci. Technol.* **2006**, 40, 1942–1949.
- (30) Scally, S.; Zhang, H.; Davison, W. Measurement of lead complexation with organic ligands using DGT. *Aust. J. Chem.* **2004**, 57, 925–930.
- (31) Gimpel, J.; Zhang, H.; Davison, W.; Edwards, A. D. In situ trace metal speciation in lake surface waters using DGT, dialysis and filtration. *Environ. Sci. Technol.* **2003**, 37, 138–146.
- (32) Downard, A. J.; Panther, J.; Kim, Y. C.; Powell, K. J. Lability of metal ion-fulvic acid complexes as probed by FIA and DGT: a comparative study. *Anal. Chim. Acta* **2003**, 499, 17–28.
- (33) Tipping, E. *Cation Binding by Humic Substances*; Cambridge University Press: New York, 2002.

Received for review May 19, 2006. Revised manuscript received July 24, 2006. Accepted August 2, 2006.

ES061215X